Dyes and Pigments 194 (2021) 109587

Contents lists available at ScienceDirect

Dyes and Pigments

journal homepage: www.elsevier.com/locate/dyepig

Design and synthesis of a novel "turn-on" fluorescent probe based on benzofuran-3(2H)-one for detection of hydrazine in water samples and biological systems

Kai Wang [a,1], Ya-Xi Ye [a,1], Cheng-Yan Jiang [b], Meng-Ya Guo [a], Xiang-Yang Zhang [a], Ai-Qin Jiang [b,**], Yu-Shun Yang [a,***], Qing-Cai Jiao [a,****], Hai-Liang Zhu [a,*]

[a] State Key Laboratory of Pharmaceutical Biotechnology, School of Life Sciences, Nanjing University, Nanjing, 210023, China
[b] Center of Translational Medicine, Jiangsu Key Laboratory of Molecular Medicine, Nanjing University Medical School, Nanjing University, Nanjing, China

ARTICLE INFO

Keywords:
Hydrazine detection
Fluorescent probe
Water samples
Substitution-cyclization-elimination cascade
Biological systems

ABSTRACT

Hydrazine is a very important industrial chemical with high toxicity to the human body. In this work, a fluorescent probe **HZ**, based on the substitution-cyclization-elimination cascade which initiated by hydrazine, was designed and synthesized. **HZ** had various characteristics such as high selectivity, high sensitivity, fast detection speed, wide application range, and so on. After treating with hydrazine, the fluorescence signal of **HZ** at 520 nm in aqueous solution was significantly enhanced. Furthermore, **HZ** had the linear range of 1–10 equivalent for monitoring hydrazine, and the solution showed a colorless to yellow color change. In practical application, the detection limit of **HZ** for the detection of hydrazine was only 0.75 μM, which could be utilized for trace detection of hydrazine in different water samples. These indicated that **HZ** had a broad application prospect in the fields of environmental protection and water treatment. This work not only provided a useful instrument for the detection of the ecological environment but also supplied important information for the system optimization of other ecological environment detectors. In addition, **HZ** could monitor endogenous and exogenous hydrazine in MCF-7 cells successfully, which demonstrated its potential for practical application in complex biological systems.

1. Introduction

As a significant industrial chemical, hydrazine is widely used in pharmaceutical, chemical, catalytic, agricultural, and other fields [1–4]. Nevertheless, due to the wide application of hydrazine, it is easy to cause environmental pollution in the whole industrial process, such as production, disposal, and so on [5]. In addition, due to its highly explosive, hydrazine plays a more crucial role in the high-energy fuel of rocket and fuel cell propulsion systems [6,7]. Hydrazine is also a highly toxic substance, which may lead to acute damage to many organs of the human body, such as the kidney, lung, and liver [8–10].

As we know, US Environmental Protection Agency (EPA) has used hydrazine as a potential carcinogen, and the threshold limit value (TLV) is 10 ppb [11]. Consequently, the trace detection of extremely harmful hydrazine has aroused great interest, and it is particularly important to control the concentration of hydrazine in industrial areas as well as to monitor the concentration of hydrazine in biological systems and drinking water [12].

At present, a variety of hydrazine detection methods have been developed, such as titrimetry [13], spectrophotometry [14], electrochemistry [15], chromatography-mass spectrometry [16,17], Raman spectroscopy [18] and so on. Unfortunately, these methods have some shortcomings, such as high cost, tedious operation, or long analysis time, which hinder the roles of these methods in practical application. In recent years, fluorescent probes have been widely developed in the detection of small molecular targets because of their sensitivity, selectivity, and good biocompatibility [19,20]. Up to now, based on the strong nucleophilic property of hydrazine, several fluorescent probes of

* Corresponding authors.
** Corresponding author.
*** Corresponding authors.
**** Corresponding author.
E-mail addresses: jianaq@nju.edu.cn (A.-Q. Jiang), ys_yang@nju.edu.cn (Y.-S. Yang), jiaoqc@nju.edu.cn (Q.-C. Jiao), zhuhl@nju.edu.cn (H.-L. Zhu).
[1] Both authors contributed equally to the work.

https://doi.org/10.1016/j.dyepig.2021.109587
Received 21 April 2021; Received in revised form 16 June 2021; Accepted 21 June 2021
Available online 22 June 2021

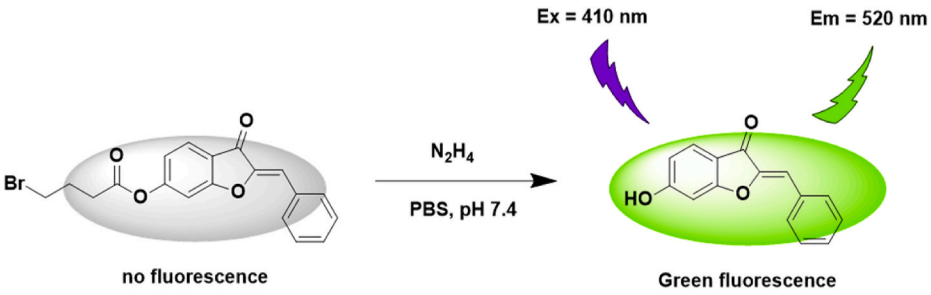

Fig. 1. The selective detection of **HZ** for hydrazine.

hydrazine have been exploited [21–23]. These fluorescent probes connected the fluorophores with the recognition groups, which was commonly the nucleophilic reaction site. The reported recognition groups of hydrazine mainly included acetyl [24–28], levulinate [29,30], 4-bromo butyrate [31–33], phthalimide [34–36], aldehyde [37], cyano group [38,39], and so on. Nevertheless, most of the hydrazine fluorescent probes had some disadvantages, such as strong background signal, negative selectivity, high cytotoxicity, and complex synthesis process. These disadvantages limited the scope of applications of the probes greatly, thus much attention has been paid to design fluorescence probes with better selectivity and higher sensitivity for the detection of hydrazine. It is believed that with the continuous improvement of selectivity and sensitivity in future research, the applications of hydrazine probes in various fields will face new opportunities and challenges.

As far as we know, benzofuranone and its derivatives have attracted much attention because of their excellent photo-physical properties, high fluorescence quantum yield, and photo bleaching resistance among many organic fluorophores. These favorable properties make benzofuranone become a powerful platform for the development of fluorescent probes for a variety of targets. Herein, we designed and synthesized a novel fluorescent probe **HZ** based on benzofuranone for monitoring of hydrazine (Fig. 1). Compared with other species, **HZ** had higher selectivity for hydrazine, and it could be used for detecting hydrazine in a variety of samples. With the addition of hydrazine, the 4-bromo butyrate group of **HZ** was replaced by hydrazine nucleophilic substitution into the corresponding hydrazone. Then the electron of the N atom attacked the C positive ion in the C═O double bond, which affected the distribution of intramolecular electron density. Finally, the fluorophore of benzofuranone derivative was formed by cyclization and elimination reaction. As a result, there were significant changes in the absorption and fluorescence spectra of **HZ**. In Table S1, we listed the previously reported probes for hydrazine and compared the properties including response time, excitation/emission wavelength, detection limit, and biological imaging capabilities [3,5,12,19,22–25,33,36,39–52]. Compared with some other hydrazine probes [49], the response time of **HZ** was short (<7 min), which was conducive to the rapid detection. In addition, because of the specificity of the recognition group 4-bromo butyrate group, **HZ** had high selectivity for hydrazine among various species than the ones with other reaction mechanisms [50]. Furthermore, **HZ** had smaller steric hindrance than other probes [33], so it was easier to adjust the excitation and emission wavelength due to its flexible structure.

In this work, the developed probe, **HZ**, had a large Stokes Shift (>110 nm) and a wide linear range (10–100 μM). Besides, **HZ** had a low proportion of DMSO (1% DMSO), which was more suitable for biological applications. Meanwhile, the limit of detection (LOD) was determined to be 0.75 μM. Given the above characteristics, we applied the probe to the rapid measurement of hydrazine in environmental water samples. In addition, **HZ** could penetrate living cells, which enabled us to use the probe for confocal imaging of hydrazine in MCF-7 cells successfully.

2. Experimental section

2.1. Materials and instruments

The chemicals reagents were commercially acquired from Aladdin Reagents. Chromatographic purification was performed using 300–400 mesh chromatography silica gel (Haiyang, Qingdao, P.R. China). All amino acids were obtained from Sigma-Aldrich. The fluorescence spectra were carried out on Hitachi F-7000 spectrophotometer. UV–vis spectra recording was conducted on Shimadzu UV-2550 spectrometer. The NMR spectra were acquired in Bruker DRX-600 and Advance III HD spectrometer. The Mass spectra were obtained from AB SCIEX Triple-TOF 4600. The pH detection was carried out with PHS-25 pH-meter (Shanghai Geotechnical International Trading Co. Ltd., Shanghai, P.R. China).

2.2. Synthesis of compound *1*

To a solution of 6-hydroxybenzofuran-3(2H)-one (5 mmol, 0.74 g) in dry ethanol (10 mL) was added benzaldehyde (5 mmol, 0.53 g) and sodium hydroxide (10 mmol, 0.4 g). The mixture was refluxed for 5 h until the starting compound was consumed, as determined by TLC [53,54]. After completing the reaction, the solution was cooled to room temperature and acidified to pH = 6.0 with acetic acid. To gain the precipitate, the ice water was added slowly. Finally, the residue was filtered, and the crude product was purified by silica gel column chromatography to acquire compound **1** (Yield: 0.83 g, 70%). ^{1}H NMR (600 MHz, DMSO-d_6) δ 11.26 (s, 1H), 7.96 (d, J = 7.4 Hz, 2H), 7.65 (d, J = 8.4 Hz, 1H), 7.51 (t, J = 7.5 Hz, 2H), 7.44 (t, J = 7.3 Hz, 1H), 6.82 (d, J = 1.9 Hz, 1H), 6.81 (s, 1H), 6.74 (dd, J = 8.4, 1.9 Hz, 1H). ^{13}C NMR (151 MHz, DMSO) δ 181.94, 168.46, 167.09, 147.85, 132.55, 131.53, 130.12, 129.45, 126.49, 113.57, 113.20, 110.80, 99.12. HRMS (ESI-TOF) *m/z*: $[M+H]^+$ Calcd. for $C_{15}H_{10}O_3$ 239.0663, Found 239.0699.

2.3. Synthesis of probe *HZ*

4-dimethylaminopyridine (DMAP) (40 mg, 0.32 mmol), 1-ethyl-3-(3-dimethylaminopropyl) carbodiimide hydrochloride (EDC·HCl) (202 mg, 1.04 mmol) and 4-bromobutyric acid (120 mg, 0.72 mmol) were dissolved into 40 mL anhydrous DCM with compound **1** [33,49]. At room temperature, the mixture was stirred for 16 h. After the reaction completed, the solvent was removed, and the residue was purified by eluting with (PE/EA = 50/1, v/v) to afford probe **HZ** (Yield: 181 mg, 65%). ^{1}H NMR (600 MHz, DMSO-d_6) δ 8.00 (d, J = 7.3 Hz, 2H), 7.87 (d, J = 8.3 Hz, 1H), 7.55–7.50 (m, 3H), 7.48 (t, J = 7.3 Hz, 1H), 7.14 (dd, J = 8.3, 1.9 Hz, 1H), 6.97 (s, 1H), 3.66 (t, J = 6.6 Hz, 2H), 2.82 (t, J = 7.3 Hz, 2H), 2.25–2.17 (m, 2H). ^{13}C NMR (151 MHz, DMSO) δ 182.90, 170.86, 166.58, 157.82, 147.21, 131.90, 130.67, 129.53, 125.86, 119.11, 118.82, 112.87, 107.83, 34.31, 32.71, 27.91. HRMS (ESI-TOF) *m/z*: $[M+H]^+$ Calcd. for $C_{19}H_{15}BrO_4$ 387.0217, Found 387.0217.

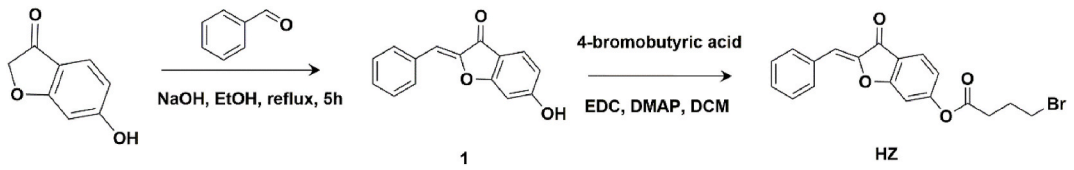

Scheme 1. The synthetic route of probe **HZ**.

2.4. Fluorescent spectral measurement

The stock solution of **HZ** (1.0 mM) was dissolved in DMSO, and other concentrations were obtained by dilution. The stock solution of hydrazine, amino acids, cations, and anions was prepared in ultrapure water. The mixture reaction solution was implemented at 37 °C for 7 min, and the fluorescence intensity was recorded. The wavelength of excitation was set as 410 nm. Both excitation and emission slit widths were 5 nm. The photomultiplier voltage was 600 V. The error bars were the standard deviation based on three independent experiments.

2.5. Determination of the fluorescence quantum yield

The fluorescence quantum yield Φ_u was detected by the relative contrast, with rhodamine B of the ethanol solution as the standard substance. Participation ratio method was recruited with the formula: $\Phi_u = [(A_s F_u n^2)/(A_u F_s n_0^2)]\Phi_s$. Herein, rhodamine B was used as control. Φ_u and Φ_s were the fluorescence quantum yields of **HZ** and reference, respectively. A_u and A_s were the absorbance values of **HZ** and reference, while F_u and F_s were their integrations of emission band areas. n and n_0 were the solvent refractive indexes of **HZ** solution and reference, respectively.

Control: $\Phi_s = 0.69$, $A_s = 0.024$, $F_s = 71.29$, $n_0 = 1.361$; For 1: Au1 = 0.038, Fu1 = 84.11, n1 = 1.477; Φu1 = 0.61; For **HZ**: $A_{u2} = 0.043$, $F_{u2} = 14.75$, $n_2 = 1.477$; $\Phi_{u2} = 0.09$;

2.6. Preparation for water samples

The stock solution of hydrazine (10 mM) was dissolved in rice water, tap water, and distilled water. A calculated amount of hydrazine, **HZ**, and PBS was added to a vial and the complex solution was diluted to 200 μL with rice water, tap water, and distilled water. The final **HZ** and hydrazine concentrations were 1.0×10^{-5} M, 0–10.0×10^{-5} M, respectively. All measurements were performed in triplicate.

2.7. MTT assay

Cell viability was performed using MCF-7 cells and HeLa cells. MCF-7 cells and HeLa cells were seeded in the medium, which was incubated with different concentrations of **HZ** at 37 °C. After 24 h, each well was added with 5 μL MTT (5 mg/mL) and placed for 4 h in the incubator at 37 °C, and then cell supernatant was removed. Finally, to each well was added 150 μL DMSO and cell viability assay was detected on Tecan Microplate Reader. The error bars were the standard deviation based on three independent experiments.

2.8. Cell culture and imaging

MCF-7 cells were cultivated with Dulbecco's Modified Eagle Medium (DMEM) (Gibco Company, USA) containing 1% Penicillin-Streptomycin and 10% FBS (Fetal Bovine Serum) in the incubator for 24 h. For the control group, MCF-7 cells were directly incubated with **HZ** (10 μM) at 37 °C for 60 min. For the experimental group, MCF-7 cells were initially treated with isoniazid (100 μM) or hydrazine (100 μM or 200 μM) at 37 °C for 30 min. Then, MCF-7 cells were incubated with **HZ** (10 μM) at 37 °C for 60 min. All confocal imaging results were completed using a single-photon confocal fluorescence microscope (Olympus FV3000). Excited at 410 nm, green fluorescence was collected from 460 to 550 nm.

3. Results and discussion

3.1. Characterization of compound 1 and probe HZ

The synthetic route of compound **1** and probe **HZ** was displayed in Scheme 1. To ensure the accuracy of the synthesis, the structures of compound **1** and probe **HZ** were confirmed by ^{1}H NMR, ^{13}C NMR, and HRMS (Figs. S6–S11).

3.2. The absorption spectrum and fluorescence spectrum response

To determine the response activity of **HZ** to hydrazine, the absorption spectrum and fluorescence spectrum were investigated at 37 °C in PBS buffer (10 mM, pH 7.4). Consequently, we monitored the UV–Vis absorption of **HZ** without and with hydrazine in PBS buffer for the first time. As seen in Fig. 2a, the UV–Vis absorption of **HZ** showed a weak absorption peak at 390 nm, while the absorbance shifted to an obvious absorption peak at 400 nm after **HZ** reacted with 500 μM hydrazine. This result implicated that **HZ** had an optical response to hydrazine. In addition, free probe **HZ** showed a very weak fluorescence emission signal due to the effective quenching effect in the absence of hydrazine. On the contrary, after being treated with hydrazine in PBS buffer, a

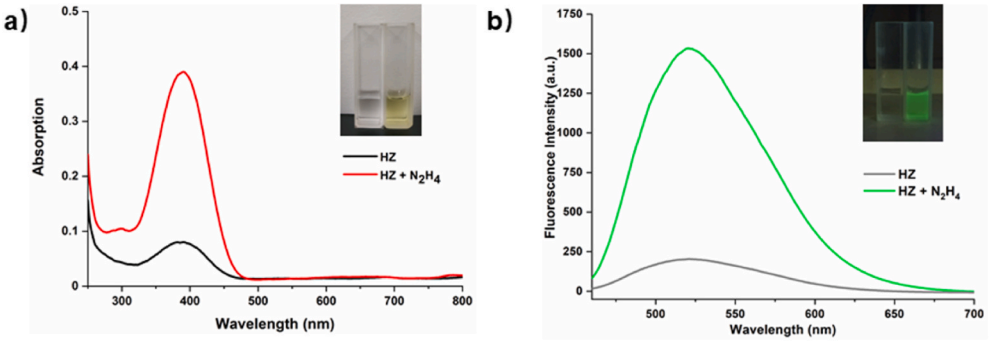

Fig. 2. a) The absorption spectra of **HZ** (10 μM) without (black) and with (red) hydrazine (500 μM). Inset (a): The images of absorption were **HZ** (10 μM) without (white) or with (yellow) hydrazine (500 μM) in visible light. b) The fluorescence spectra of **HZ** (10 μM) without and with hydrazine (500 μM) for 7 min at 37 °C. Insert (b): The different colors without (left) and with hydrazine (right) under UV 365 nm. Excitation: 410 nm; Slit widths: 5 nm*5 nm; Photomultiplier voltage: 600 V.

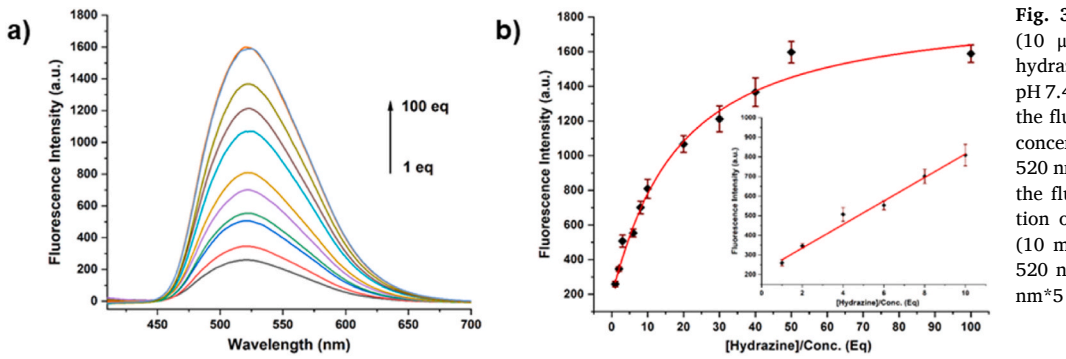

Fig. 3. a) The fluorescence spectra of **HZ** (10 μM) with different concentrations of hydrazine (1–100 eq) in PBS buffer (10 mM, pH 7.4, 1% DMSO) for 7 min. b) The curve of the fluorescence intensity with the different concentrations of hydrazine (1–100 eq) at 520 nm. Insert (b): The linear relationship of the fluorescence signal with the concentration of hydrazine (1–10 eq) in PBS buffer (10 mM, pH 7.4, 1% DMSO) for 7 min at 520 nm. Excitation: 410 nm; Slit widths: 5 nm*5 nm; Photomultiplier voltage: 600 V.

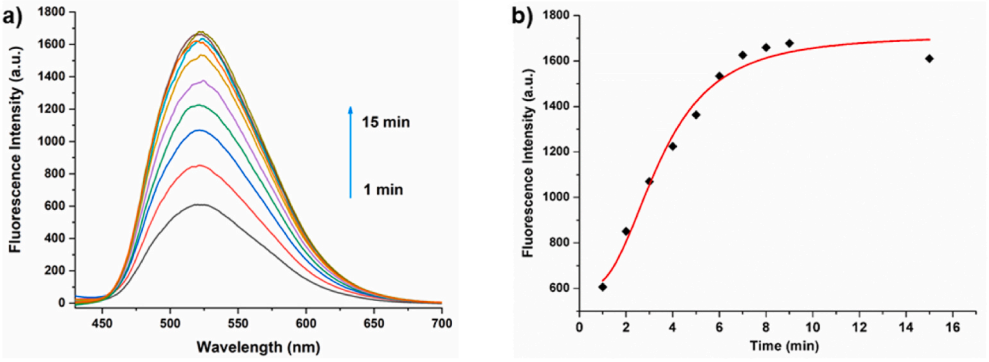

Fig. 4. a) and b) Time-dependent fluorescence intensity of **HZ** incubated with hydrazine (500 μM) in PBS buffer (10 mM, 1% DMSO, pH 7.4) at 37 °C for different time (1–15 min). Excitation: 410 nm; Slit widths: 5 nm*5 nm; Photomultiplier voltage: 600 V.

remarkable fluorescence signal emerged at 520 nm (Fig. 2b). These results showed that hydrazine could expose the fluorophore and release bright green fluorescence intensity (Fig. 2b insert), which significantly increased through nucleophilic substitution, cyclization, and elimination reaction. Furthermore, **HZ** was seemly an ideal detector for monitoring hydrazine *in vitro*.

According to the practical properties of **HZ** towards hydrazine, we carried out the following fluorescent determination experiment. The fluorescence quantum yield of **HZ** was calculated as 0.09, which showed that **HZ** had a certain real value as a turn-on probe. As seen in Fig. 3a, the fluorescence signal of **HZ** (10 μM) enhanced gradually at 520 nm when incubated with different concentrations of hydrazine (1–100 eq). When the concentration of hydrazine was added to 50.0 equivalent (500 μM), the fluorescence intensity reached the plateau (Fig. 3b). To better quantify the content of hydrazine in various samples, we explored the quantitative linear range of hydrazine by **HZ**. We found that when the concentration of hydrazine was in the range of 1–10.0 equivalent, the fluorescence intensity of **HZ** raised linearly at 520 nm. Finally, with the continuous dilution of hydrazine concentration, we found that the detection limit of hydrazine was 0.75 μM (Fig. 3b insert).

3.3. *pH-Titration and time-dependent curve*

We first investigated the fluorescence intensity changes of **HZ** with different pH in the absence and presence of hydrazine. It could be seen that when hydrazine was not added, the fluorescence intensity of **HZ** was almost unchanged within the pH range of 3–9. With the addition of hydrazine, the fluorescence intensity of **HZ** was significantly enhanced within the pH range of 6–9 (Fig. S1). The above results showed that **HZ** could monitor the level of hydrazine in physiological conditions.

To investigate the response time of **HZ**, we measured the time-dependent fluorescence intensity changes of **HZ** in PBS buffer. As

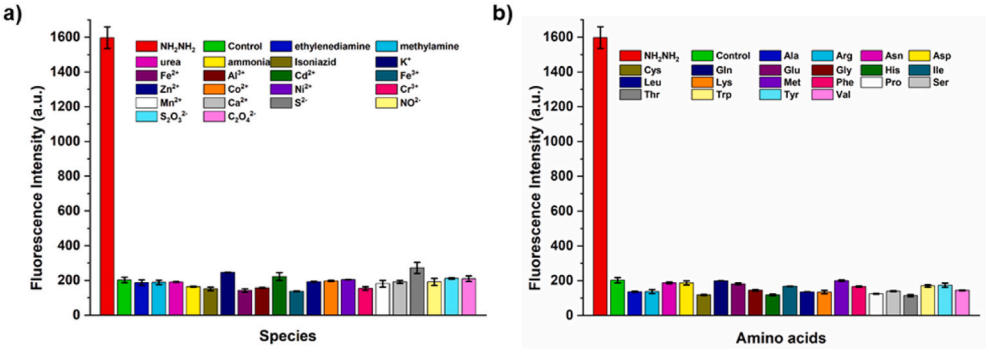

Fig. 5. a) The fluorescence signal of the **HZ** (10 μM) with different species (1 mM) in PBS buffer (10 mM, 1% DMSO, pH 7.4) for 7 min at 520 nm. b) The fluorescence signal of the **HZ** (10 μM) with different amino acids (1 mM) in PBS buffer (10 mM, 1% DMSO, pH 7.4) for 7 min at 520 nm. Excitation: 410 nm; Slit widths: 5 nm*5 nm; Photomultiplier voltage: 600 V.

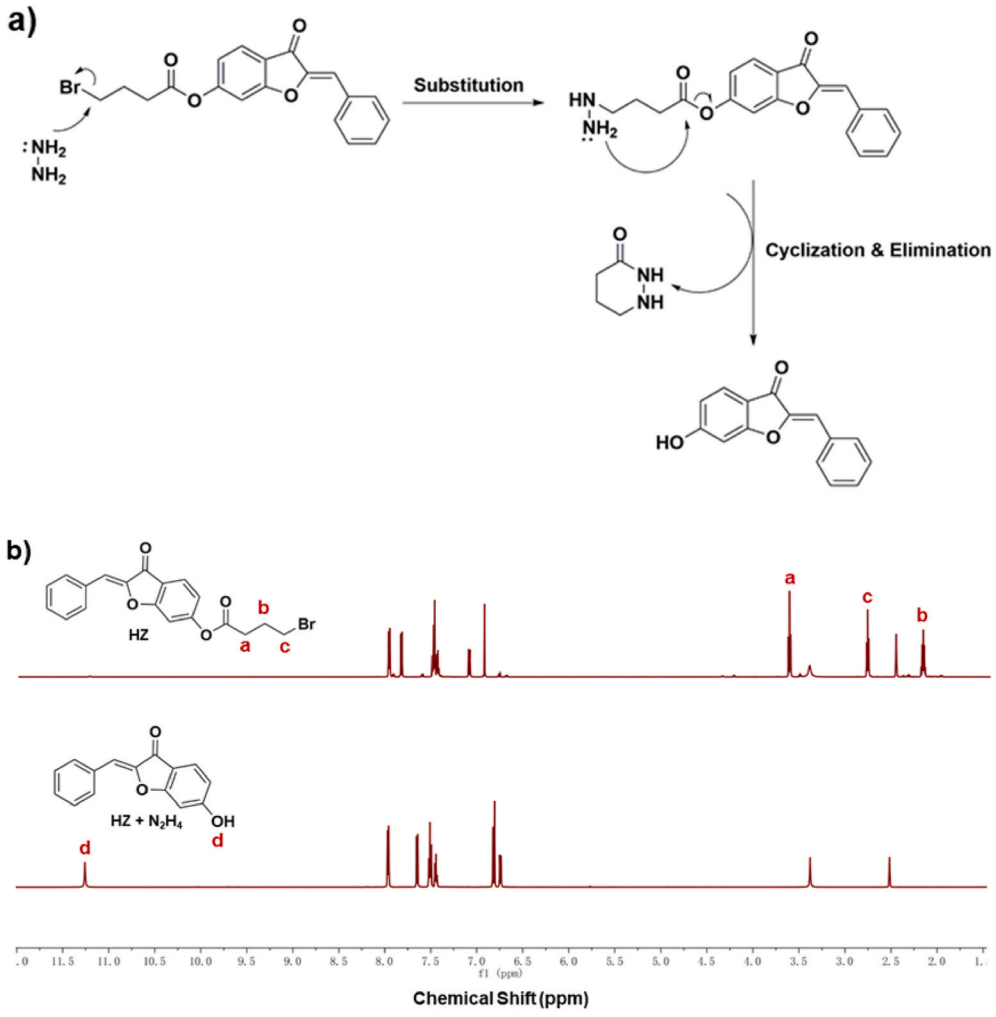

Fig. 6. a) The plausible mechanism b) the NMR spectra for hydrazine of **HZ**.

shown in Fig. 4a and b, when hydrazine was added, the fluorescence signal increased significantly and reached a plateau within 7 min. The shorter reaction time was more beneficial for the rapid determination of hydrazine. Herein, 7 min was selected as the reaction time.

3.4. Selectivity analysis

The selectivity of **HZ** was significant in the determination of hydrazine, so we evaluated the selectivity of **HZ** with the addition of various analytes (Fig. 5a and b). The analytes mainly included compounds ethylenediamine, methylamine, urea, ammonia, isoniazid, metal ions K^{+}, Fe^{2+}, Al^{3+}, Cd^{2+}, Fe^{3+}, Zn^{2+}, Co^{2+}, Ni^{2+}, Cr^{3+}, Mn^{2+}, Ca^{2+}, anions S^{2-}, NO^{2-}, $S_2O_3^{2-}$, $C_2O_4^{2-}$, and amino acids Ala, Arg, Asn, Asp, Cys, Gln, Glu, Gly, His, Ile, Leu, Lys, Met, Phe, Pro, Ser, Thr, Trp, Tyr, Val. In Fig. 5, we found that there was no obvious fluorescence enhancement in all groups except for hydrazine, and the color of the

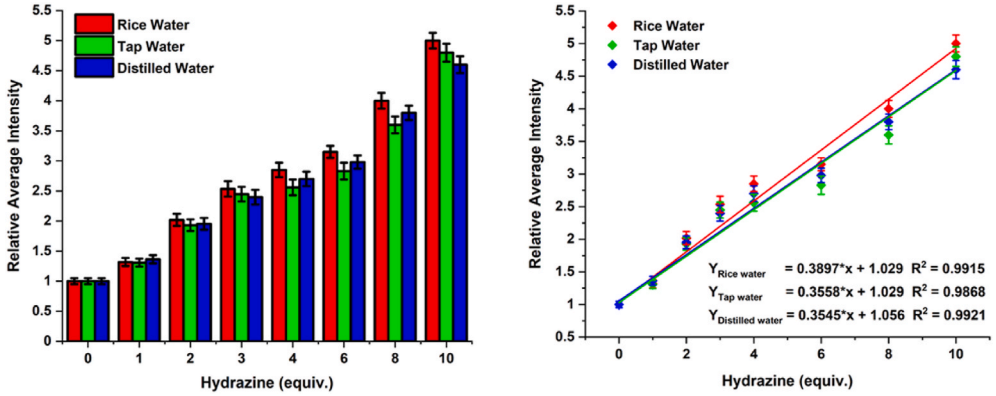

Fig. 7. a) The fluorescence intensity of **HZ** (1.0×10^{-5} M) with the concentration of hydrazine in rice water, tap water, and distilled water. b) The linear relationship of the fluorescence intensity with the concentration of hydrazine (0–10.0×10^{-5} M) in rice water, tap water, and distilled water. Excitation: 410 nm; Slit widths: 5 nm*5 nm; Photomultiplier voltage: 600 V.

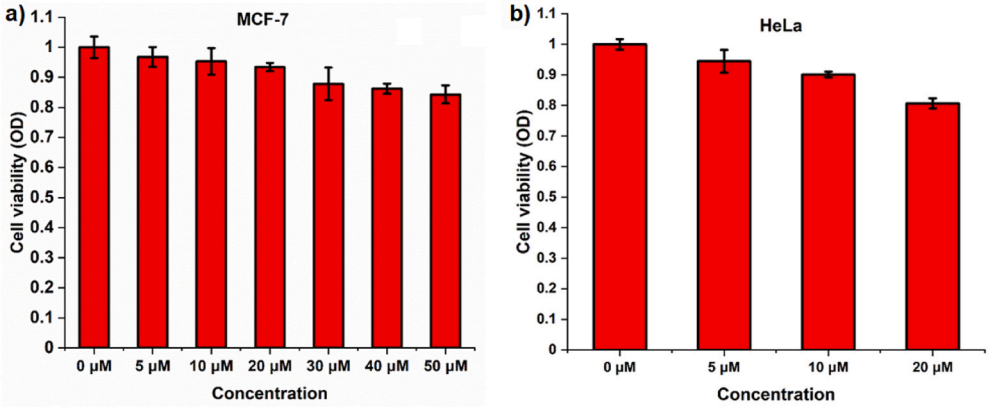

Fig. 8. Cell viability of a) MCF-7 and b) HeLa with different concentrations of **HZ** for 24 h.

solution did not change with the addition of different analytes. These results indicated that the selectivity of **HZ** was good. The excellent selectivity of **HZ** made it more suitable for the detection of hydrazine in complex biological systems.

3.5. Reaction mechanism study of *HZ*

The deprotection method of 4-bromo butyrate quenching fluorophore was used here. In **HZ**, 4-bromo butyric acid was the reaction site of hydrazine. When hydrazine was added, the 4-bromo butyric acid group of **HZ** was replaced by hydrazine nucleophilic substitution into the corresponding hydrazone. Then the electron of the N atom attacked the C positive ion in the C═O double bond, which affected the distribution of intramolecular electron density. Finally, the fluorophore of benzofuranone derivatives was formed by cyclization and elimination reaction (Fig. 6a). The NMR spectra and MS spectra analyses have verified the mechanism (Figs. 6b and S2). In addition, to better explain the reaction mechanism, the ^{1}H NMR, ^{13}C NMR, and HRMS of the reaction product after purification were provided (Figs. S3–S5).

3.6. Detection of hydrazine in water samples

Hydrazine is an important detection index in the process of environmental protection and water treatment, so the detection of hydrazine in water samples has attracted wide attention. The hydrazine in rice water, tap water, and distilled water were monitored by **HZ**. There was no obvious fluorescence enhancement in the detected water samples without hydrazine after incubating with **HZ**. However, the water

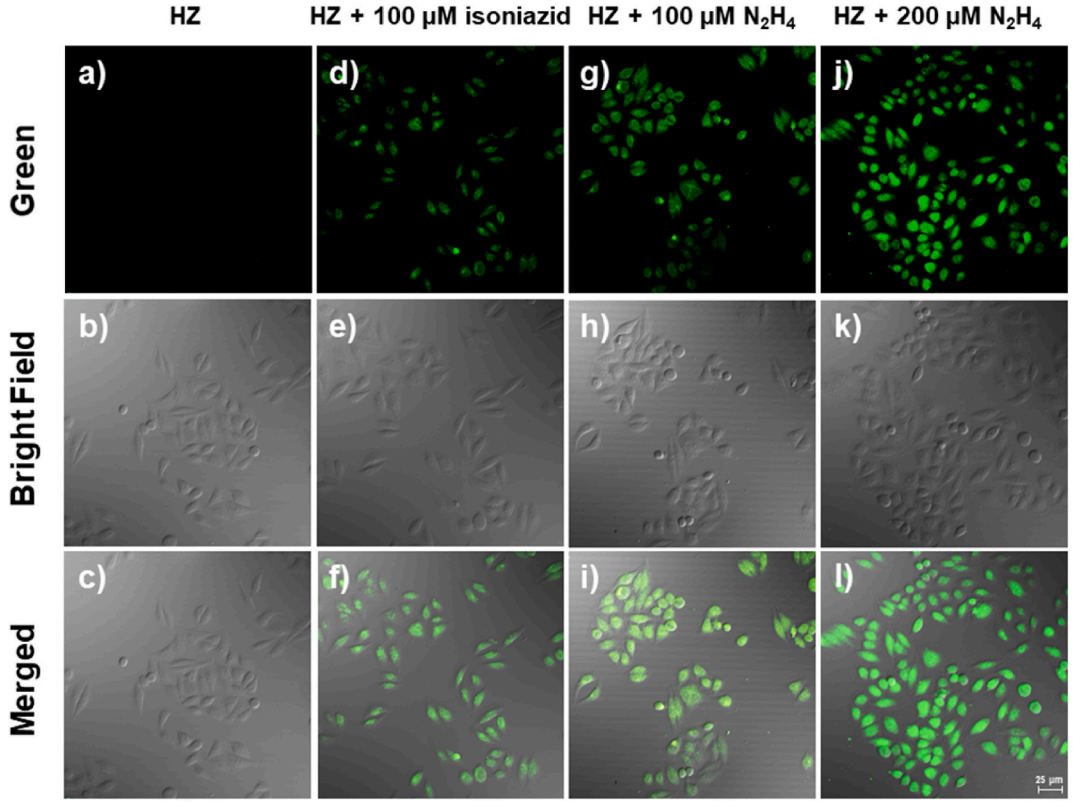

Fig. 9. The fluorescent images of MCF-7 cells with **HZ** under different treatments. (a–c) Control: the cells were treated with **HZ** (10 μM) for 60 min at 37 °C; (d–l) Others: the cells were firstly treated with isoniazid (100 μM), hydrazine (100 μM or 200 μM) for 30 min at 37 °C, then incubated with **HZ** (10 μM) for 60 min at 37 °C. Scale bar: 25 μm.

samples were treated with different hydrazine concentrations (0–10.0 × 10^{-5} M) and appeared sharp fluorescence signals after incubating with **HZ**. As shown in Fig. 7a, the recoveries gained by **HZ** intensity were compared, which indicated that **HZ** had practical value for monitoring hydrazine in different water samples. In addition, to better research the content of hydrazine in different water samples, we explored the quantitative linear range of hydrazine by **HZ** with the fluorescence intensity (Fig. 7b). The results showed that **HZ** could quantify hydrazine in various water samples.

3.7. Detection of hydrazine in live cells

Before imaging cells, we firstly used MTT assay to determine the cytotoxicity of **HZ** on MCF-7 cells and HeLa cells. The results showed that even if the concentration of **HZ** increased to more than 50 μM, the survival rate of MCF-7 cells was still above 80% (Fig. 8a). The cytotoxicity of **HZ** in HeLa cells was also relatively low (Fig. 8b). We demonstrated that the toxicity of **HZ** was low, which provided a good basis for subsequent cell experiments.

Encouraged by the above results of good cytotoxicity of **HZ**, we investigated the biological practical value of **HZ** in living cells by Olympus FV3000 confocal microscope. The confocal experiment was used to evaluate the cell permeability and imaging ability of **HZ** in MCF-7 cells. In the control group, **HZ** was incubated with MCF-7 cells at 37 °C for 60 min directly and then photographed. As shown in Fig. 9a–c, it was no obvious fluorescence in the green channel excited by 410 nm. In the experimental group, MCF-7 cells were initially incubated with 100 μM isoniazid for 30 min and then treated with **HZ** for 60 min, which did show a bright fluorescence emission signal (Fig. 9d–f). The above results showed that isoniazid could induce the production of endogenous hydrazine in living cells.

In the other groups, MCF-7 cells were initially incubated with 100 μM or 200 μM hydrazine for 30 min and then treated with **HZ** for 60 min, which displayed a bright fluorescence emission signal (Fig. 9g–l). The results showed that the fluorescence intensity of the 200 μM group was significantly higher than that of the 100 μM group in the green channel. Thus, there was a dose-dependent fluorescence enhancement. The good cell morphology further proved the strong cell membrane permeability of **HZ**. The results showed that **HZ** was compatible with the measurement of hydrazine in living cells, and its advantages were mainly reflected in low cytotoxicity and good biocompatibility. The above results showed that **HZ** could monitor endogenous and exogenous hydrazine in living cells.

4. Conclusion

In summary, a novel benzofuranone-derivated fluorescent probe **HZ** for detecting hydrazine was exploited. The results indicated that **HZ** reacted with hydrazine (<7 min) rapidly. Furthermore, **HZ** had a significant enhancement of fluorescence signal at 520 nm in the presence of hydrazine. The linear correlation was applicable for quantifying hydrazine (1.0–10.0 equiv. to cover 10–100 μM), and the limit of detection was 0.75 μM. In addition to the above advantages, **HZ** also had higher selectivity for hydrazine, which could be used for the monitoring of hydrazine in complex biological systems. Additionally, **HZ** could meet the requirements for the detection of hydrazine in natural water sources because it could work within the range of pH 6–9. **HZ** could be successfully applied to the fluorescence imaging of endogenous and exogenous hydrazine in living cells, which was attributed to the good cell membrane permeability and low cytotoxicity of **HZ**. We have reason to believe that **HZ** will become a potential tool for the detection of hydrazine in biology and the environment in the near future.

Declaration of competing interest

The authors declare that they have no known competing financial interests or personal relationships that could have appeared to influence the work reported in this paper.

Acknowledgment

We would like to thank M.S. Xin-Yue Chen for technical assistance in the preparation of the paper. This work was supported by the Major Science and Technology Program for Water Pollution Control and Treatment, China (No. 2017ZX07602-002).

Appendix A. Supplementary data

Supplementary data to this article can be found online at https://doi.org/10.1016/j.dyepig.2021.109587.

References

[1] Tan Y, Yu J, Gao J, Cui Y, Yang Y, Qian G. A new fluorescent and colorimetric probe for trace hydrazine with a wide detection range in aqueous solution. Dyes Pigments 2013;99:966–71.
[2] Ramakrishnam Raju MV, Chandra Prakash E, Chang H-C, Lin H-C. A facile ratiometric fluorescent chemodosimeter for hydrazine based on Ing-Manske hydrazinolysis and its applications in living cells. Dyes Pigments 2014;103:9–20.
[3] Liu B, Liu Q, Shah M, Wang J, Zhang G, Pang Y. Fluorescence monitor of hydrazine *in vivo* by selective deprotection of flavonoid. Sensor Actuator B Chem 2014;202:194–200.
[4] Sun Y, Zhao D, Fan S, Duan L. A 4-hydroxynaphthalimide-derived ratiometric fluorescent probe for hydrazine and its *in vivo* applications. Sensor Actuator B Chem 2015;208:512–7.
[5] Li Z, Zhang W, Liu C, Yu M, Zhang H, Guo L, Wei L. A colorimetric and ratiometric fluorescent probe for hydrazine and its application in living cells with low dark toxicity. Sensor Actuator B Chem 2017;241:665–71.
[6] Bando K, Kunimatsu T, Sakai J, Kimura J, Funabashi H, Seki T, Bamba T, Fukusaki E. GC-MS-based metabolomics reveals mechanism of action for hydrazine induced hepatotoxicity in rats. J Appl Toxicol 2011;31:524–35.
[7] Lan R, Irvine JTS, Tao S. Ammonia and related chemicals as potential indirect hydrogen storage materials. Int J Hydrogen Energy 2012;37:1482–94.
[8] Garrod S, Bollard ME, Nicholls AW, Connor SC, Connelly J, Nicholson JK, Holmes E. Integrated metabonomic analysis of the multiorgan effects of hydrazine toxicity in the rat. Chem Res Toxicol 2005;18:115–22.
[9] Yang Y, Liu X, Yan D, Deng P, Guo Z, Zhan H. Europium ion post-functionalized zirconium metal-organic frameworks as luminescent probes for effectively sensing hydrazine hydrate. RSC Adv 2018;8:17471–6.
[10] Tahira A, Nafady A, Baloach Q, Sirajuddin, Sherazi STH, Shaikh T, Arain M, Willander M, Ibupoto ZH. Ascorbic acid assisted synthesis of cobalt oxide nanostructures, their electrochemical sensing application for the sensitive determination of hydrazine. J Electron Mater 2016;45:3695–701.
[11] Zhao XX, Zhang JF, Liu W, Zhou S, Zhou ZQ, Xiao YH, Xi G, Miao JY, Zhao BX. A unique dansyl-based chromogenic chemosensor for rapid and ultrasensitive hydrazine detection. J Mater Chem B 2014;2:7344–50.
[12] Paul S, Nandi R, Ghoshal K, Bhattacharyya M, Maiti DK. A smart sensor for rapid detection of lethal hydrazine in human blood and drinking water. New J Chem 2019;43:3303–8.
[13] Burns EA, Lawler EA. Determination of mixtures of hydrazine and 1,1-Dimethylhydrazine (UDMH). Anal Chem 1963;35:802–6.
[14] Collins GE, Rose-Pehrsson SL. Fluorescent detection of hydrazine, monomethylhydrazine, and 1,1-dimethylhydrazine by derivatization with aromatic dicarbaldehydes. Analyst 1994;119:1907–13.
[15] Daemi S, Ashkarran AA, Bahari A, Ghasemi S. Fabrication of a gold nanocage/graphene nanoscale platform for electrocatalytic detection of hydrazine. Sensor Actuator B Chem 2017;245:55–65.
[16] Sun M, Bai L, Liu DQ. A generic approach for the determination of trace hydrazine in drug substances using *in situ* derivatization-headspace GC-MS. J Pharmaceut Biomed Anal 2009;49:529–33.
[17] Zhao Y, Qiu W, Yang C, Wang J. Study on a novel oxidation process for removing arsenic from flue gas. Energy Fuel 2016;31:693–8.
[18] Gu X, Camden JP. Surface-enhanced Raman spectroscopy-based approach for ultrasensitive and selective detection of hydrazine. Anal Chem 2015;87:6460–4.
[19] Qian Y, Lin J, Han L, Lin L, Zhu H. A resorufin-based colorimetric and fluorescent probe for live-cell monitoring of hydrazine. Biosens Bioelectron 2014;58:282–6.
[20] Zhai Q, Feng W, Feng G. Rapid detection of hydrazine in almost wholly water solution and in living cells with a new colorimetric and fluorescent turn-on probe. Anal. Methods-UK 2016;8:5832–7.
[21] Zhou J, Shi R, Liu J, Wang R, Xu Y, Qian X. An ESIPT-based fluorescent probe for sensitive detection of hydrazine in aqueous solution. Org Biomol Chem 2015;13:5344–8.
[22] Samanta SK, Maiti K, Ali SS, Guria UN, Ghosh A, Datta P, Mahapatra AK. A solvent directed D-π-A fluorescent chemodosimeter for selective detection of hazardous hydrazine in real water sample and living cell. Dyes Pigments 2020;173. Article Number 107997.

[23] Li J, Cui Y, Bi C, Feng S, Yu F, Yuan E, Xu S, Hu Z, Sun Q, Wei D, Yoon J. Oligo (ethylene glycol)-functionalized ratiometric fluorescent probe for the detection of hydrazine *in vitro* and *in vivo*. Anal Chem 2019;91:7360–5.
[24] Hu C, Sun W, Cao J, Gao P, Wang J, Fan J, Peng X. A ratiometric Near-Infrared fluorescent probe for hydrazine and its *in vivo* applications. Org Lett 2013;15: 4022–5.
[25] Zhang J, Ning L, Liu J, Wang J, Yu B, Liu X, Yao X, Zhang Z, Zhang H. Naked-eye and near-infrared fluorescence probe for hydrazine and its applications in *in vitro* and *in vivo* bioimaging. Anal Chem 2015;87:9101–7.
[26] Choi MG, Moon JO, Bae J, Lee JW, Chang SK. Dual signaling of hydrazine by selective deprotection of dichlorofluorescein and resorufin acetates. Org Biomol Chem 2013;11:2961–5.
[27] Liu C, Wang F, Xiao T, Chi B, Wu Y, Zhu D, Chen X. The ESIPT fluorescent probes for N_2H_4 based on benzothiazol and their applications for gas sensing and bioimaging. Sensor Actuator B Chem 2018;256:55–62.
[28] Shi X, Huo F, Chao J, Yin C. A ratiometric fluorescent probe for hydrazine based on novel cyclization mechanism and its application in living cells. Sensor Actuator B Chem 2018;260:609–16.
[29] Choi MG, Hwang J, Moon JO, Sung J, Chang SK. Hydrazine-selective chromogenic and fluorogenic probe based on levulinated coumarin. Org Lett 2011;13:5260–3.
[30] Zhu S, Lin W, Yuan L. Development of a Near-Infrared fluorescent probe for monitoring hydrazine in serum and living cells. Anal. Methods-UK 2013;5:3450–3.
[31] Goswami S, Das S, Aich K, Pakhira B, Panja S, Mukherjee SK, Sarkar S. A chemodosimeter for the ratiometric detection of hydrazine based on return of ESIPT and its application in live-cell imaging. Org Lett 2013;15:5412–5.
[32] Lu Z, Fan W, Shi X, Lu Y, Fan C. Two distinctly separated emission colorimetric NIR fluorescent probe for fast hydrazine detection in living cells and mice upon independent excitations. Anal Chem 2017;89:9918–25.
[33] Lu Z, Shi X, Ma Y, Fan W, Lu Y, Wang Z, Fan C. A simple two-output Near-Infrared fluorescent probe for hydrazine detection in living cells and mice. Sensor Actuator B Chem 2018;258:42–9.
[34] Cui L, Ji C, Peng Z, Zhong L, Zhou C, Yan L, Qu S, Zhang S, Huang C, Qian X, Xu Y. Unique tri-output optical probe for specific and ultrasensitive detection of hydrazine. Anal Chem 2014;86:4611–7.
[35] Ali F, A AH, Taye N, Mogare DG, Chattopadhyay S, Das A. Specific receptor for hydrazine: mapping the *in situ* release of hydrazine in live cells and in an *in vitro* enzymatic assay. Chem Commun 2016;52:6166–9.
[36] Zheng XX, Wang SQ, Wang HY, Zhang RR, Liu JT, Zhao BX. Novel pyrazoline-based selective fluorescent probe for the detection of hydrazine. Spectrochim Acta A 2015;138:247–51.
[37] Jung Y, Ju IG, Choe YH, Kim Y, Park S, Hyun YM, Oh MS, Kim D. Hydrazine expose: the next-generation fluorescent probe. ACS Sens 2019;4:441–9.
[38] Fan J, Sun W, Hu M, Cao J, Cheng G, Dong H, Song K, Liu Y, Sun S, Peng X. An ICT-based ratiometric probe for hydrazine and its application in live cells,. Chem Commun 2012;48:8117–9.
[39] Wu J, Pan J, Ye Z, Zeng L, Su D. A smart fluorescent probe for discriminative detection of hydrazine and bisulfite from different emission channels. Sensor Actuator B Chem 2018;274:274–84.
[40] Wu Q, Zheng J, Zhang W, Wang J, Liang W, Stadler FJ. A new quinoline-derived highly-sensitive fluorescent probe for the detection of hydrazine with excellent large-emission-shift ratiometric response. Talanta 2019;195:857–64.
[41] Qiu XY, Liu SJ, Hao YQ, Sun JW, Chen S. Phenothiazine-based fluorescence probe for ratiometric imaging of hydrazine in living cells with remarkable Stokes shift. Spectrochim Acta A 2020;227. Article Number 117675.
[42] Xu H, Gu B, Li Y, Huang Z, Su W, Duan X, Yin P, Li H, Yao S. A highly selective, colorimetric and ratiometric fluorescent probe for NH_2NH_2 and its bioimaging. Talanta 2018;180:199–205.
[43] Li K, Xu H-R, Yu K-K, Hou J-T, Yu X-Q. A coumarin-based chromogenic and ratiometric probe for hydrazine. Anal. Methods-UK 2013;5:2653–6.
[44] Liu Y, Ren D, Zhang J, Li H, Yang X-F. A fluorescent probe for hydrazine based on a newly developed 1-indanone-fused coumarin scaffold. Dyes Pigments 2019;162: 112–9.
[45] Qi YL, Chen J, Zhang B, Li H, Li DD, Wang BZ, Yang YS, Zhu HL. A turn-on fluorescent sensor for selective detection of hydrazine and its application in *Arabidopsis thaliana*. Spectrochim Acta A 2020;227. Article Number 117707.
[46] Shi X, Huo F, Chao J, Zhang Y, Yin C. An isophorone-based NIR probe for hydrazine in real water samples and hermetic space. New J Chem 2019;43:10025–9.
[47] Jin X, Liu C, Wang X, Huang H, Zhang X, Zhu H. A flavone-based ESIPT fluorescent sensor for detection of N_2H_4 in aqueous solution and gas state and its imaging in living cells. Sensor Actuator B Chem 2015;216:141–9.
[48] Xia X, Zeng F, Zhang P, Lyu J, Huang Y, Wu S. An ICT-based ratiometric fluorescent probe for hydrazine detection and its application in living cells and *in vivo*. Sensor Actuator B Chem 2016;227:411–8.
[49] Goswami S, Aich K, Das S, Basu Roy S, Pakhira B, Sarkar S. A reaction based colorimetric as well as fluorescence 'turn on' probe for the rapid detection of hydrazine. RSC Adv 2014;4:14210–4.
[50] Ma J, Fan J, Li H, Yao Q, Xia J, Wang J, Peng X. Probing hydrazine with a Near-Infrared fluorescent chemodosimeter. Dyes Pigments 2017;138:39–46.
[51] Song Y, Chen G, Han X, You J, Yu F. A highly sensitive Near-Infrared ratiometric fluorescent probe for imaging of mitochondrial hydrazine in cells and in mice models. Sensor Actuator B Chem 2019;286:69–76.
[52] Wang S, Ma S, Zhang J, She M, Liu P, Zhang S, Li J. A highly sensitive and selective Near-Infrared fluorescent probe for imaging hydrazine in living tissues and mice. Sensor Actuator B Chem 2018;261:418–24.
[53] Fang L, Zhang X-Y, Yuan Q, Li D-D, Jiao Q-C, Yang Y-S, Zhu H-L. A novel indanone-derivated fluorescence sensor for Cysteine detection and biological imaging. Dyes Pigments 2020;175. Article Number 108122.
[54] Ren TB, Xu W, Zhang QL, Zhang XX, Wen SY, Yi HB, Yuan L, Zhang XB. Enhancing the anti-solvatochromic two-photon fluorescence for cirrhosis imaging by forming a hydrogen-bond network. Angew Chem Int Ed 2018;57:7473–7.